

Control of Tensile Stress in Prestressed Concrete Members Under Service Loads

Deuck Hang Lee¹⁾, Sun-Jin Han²⁾, Hyo-Eun Joo²⁾, and Kang Su Kim^{2)*} 

(Received August 22, 2017, Accepted March 14, 2018)

Abstract: In current design codes, crack control design criterion for prestressed concrete (PSC) members is stricter than conventional reinforced concrete (RC) members. In particular, it is stipulated that the net tensile stress of prestressing strands should be controlled under 250 MPa in the serviceability design of PSC members belonging to the Class C category section that is expected to be cracked due to flexure under service load conditions as defined in ACI318 code. Thus, the cracked section analysis is essentially required to estimate the tensile stress of the prestressing strands under the service loads, which requires very complex iterative calculations, thereby causing many difficulties in the applications of the Class C PSC members in practice. Thus, this study proposed a simple method to estimate the net tensile stress of the prestressing strands (Δf_{ps}) under the service load conditions, and also provided a summary table to be used for checking whether the net tensile stress (Δf_{ps}) exceeds the stress limit (250 or 350 MPa) with respect to the magnitude of effective prestress (f_{se}).

Keywords: prestressed concrete, serviceability, design code, strand, stress limit, effective prestress.

1. Introduction

The current ACI318 building code (ACI Committee 318 2014) has stipulated more conservative provisions for the crack control design of prestressed concrete (PSC) members reinforced with high strength prestressing strands compared to conventional reinforced concrete (RC) members. As shown in Fig. 1, the net tensile stress of prestressing strands in the PSC members with cracked section properties, belonging to the Class C category according to the ACI318 code, is expected to be significantly higher at the service load condition compared to that of the Class U and T categories (i.e., uncracked sections). The PSC members exhibit very different flexural behaviors at the service load level depending on the magnitude of the effective prestress (f_{se}) and the partial prestressing ratio (PPR) even when they have the same flexural strength (Kim and Lee 2011; Lee and Kim 2011; Lee et al. 2013, 2014; Park et al. 2016, 2017; Park and Cho 2017). In the ACI318-14 code, it is specified that the net tensile stress of the prestressing strands (Δf_{ps}) shall not exceed 250 MPa for the Class C PSC members to ensure proper crack control at the service loads. In order to estimate

the net tensile stress of the prestressing strands (Δf_{ps}) in the Class C flexural members under the service load conditions, the cracked section analysis should be essentially conducted, which unfortunately requires very complex and time-consuming iterative calculations, as pointed out by Skogman et al. (1988). and Mast et al. (2008). Thus, this study aims to develop a simple method to estimate the net tensile stress of the prestressing strands (Δf_{ps}) under the service load conditions. On the other hand, based on the flexural analysis results of prestressed concrete members with various sectional properties, a summary table is also proposed, which can be used to easily check whether the net tensile stress (Δf_{ps}) exceeds the specified stress limit (250 MPa) using only the magnitude of the effective prestress (f_{se}) without calculating the net tensile stress of the prestressing strands (Δf_{ps}).

2. Research Significance

In this study, nonlinear flexural analyses were performed on a total of 1248 prestressed concrete members with various sectional types, partial prestressing ratios, reinforcing indices, yield strengths of nonprestressed reinforcements, and effective prestresses, based on which a simple method was proposed to estimate the net tensile stress (Δf_{ps}) of the prestressing strands at the service loads. In order to examine whether the net tensile stress (Δf_{ps}) of the prestressing strands exceeds the limitation specified in design codes for serviceability check of the Class C PSC members, the proposed method do not require the cracked section analysis

¹⁾Department of Civil Engineering, Nazarbayev University, 53 Kabanbay Batyr Ave, Astana 010000, Republic of Kazakhstan.

²⁾Department of Architectural Engineering, University of Seoul, 163 Seoulsiripdae-ro, Dongdaemun-gu, Seoul 02504, South Korea.

*Corresponding Author; E-mail: kangkim@uos.ac.kr

Copyright © The Author(s) 2018

that involves very complex and time-consuming iterative calculations.

3. Net Tensile Stress Limit for PSC Members at Service Loads

According to the ACI318-14 design code, the stress change in prestressed reinforcements at the service loads (Δf_{ps}) shall be calculated by the cracked section analysis for the PSC members belonging to the Class C category that are cracked in flexure under service load conditions. For the purpose of a proper crack control at the service loads, the value of Δf_{ps} is limited to 250 MPa (36,000 psi) for the Class C PSC members. As mentioned in the ACI318-14 commentary R24.3.2.2, the maximum stress limit of 250 MPa for the Class C PSC member (Δf_{ps}) is intended to be similar to the maximum allowable stress of the conventional reinforced concrete (RC) members with the Grade 60 reinforcements ($f_y = 420$ MPa where f_y is the yield strength of nonprestressed reinforcement), which can be calculated as $2/3 f_y$ (i.e., 280 MPa). The ACI318-14, however, also allows the use of the Grade 80 reinforcements ($f_y = 550$ MPa), where the maximum allowable stress is estimated to be about 370 MPa, which is significantly higher than that of the RC members reinforced with the Grade 60 reinforcements (i.e., 280 MPa). On the contrary, the limit value for Δf_{ps} has been fixed for the Class C partially prestressed concrete members as 250 MPa regardless of the Grades of the nonprestressed reinforcements. This means that Δf_{ps} is, of course, limited as 250 MPa even for the PSC members reinforced with combinations of 1860 MPa strands and 550 MPa yield strength (Grade 80) rebars.

On the other hand, the cracked section analysis should be essentially conducted to estimate the net tensile stress of the PSC members with the Class C section properties, which requires quite complex iterative calculations, as described by

Mast et al. (2008), and PCI design handbook (Prestressed Concrete Institute 2010) in detail. To overcome such limitations, this study proposed a simple method to estimate the net tensile stress of the prestressing strands in the Class C PSC members at service loads (Δf_{ps}) without the iterative cracked section analysis so that the maximum spacing of the prestressing strands specified in the ACI318 code for the proper crack control can be easily calculated. In addition, this study also presented a summary table to be used for checking whether the net tensile stress (Δf_{ps}) exceeds the stress limit (250 or 350 MPa) with respect to the magnitude of effective prestress (f_{se}).

4. Parametric Study for Estimation of Net Tensile Stresses of PSC Members at Service Loads

4.1 Variables for Parametric Study

This study conducted numerous nonlinear flexural analyses on 1248 PSC members that were selected from Lee et al. (2013, 2014) and PCI Handbook (Prestressed Concrete Institute 2010), based on which this study aimed to propose a simple method for estimating the net tensile stress (Δf_{ps}) of the prestressing strands at the service loads. As shown in Table 1 and Fig. 2, the PSC members were rectangular, T-shaped, or inverted-T-shaped (IT-shaped). In the parametric study, the levels of effective prestresses were the key parameter, and various ranges of section sizes, partial prestressing ratios, reinforcing indices, and yield strengths of nonprestressed reinforcements were also included. With respect to all the prestressed concrete sections, the tensile strength of prestressing strands (f_{pu}) was 1,860 MPa (Grade 270) while two types of reinforcing bars were included; the yield strengths of reinforcing bars (f_y) were 420 and 550 MPa (Grades 60 and 80). Four levels of the effective prestress (f_{se}), i.e., $0.5 f_{pu}$, $0.55 f_{pu}$, $0.6 f_{pu}$, and $0.65 f_{pu}$, were

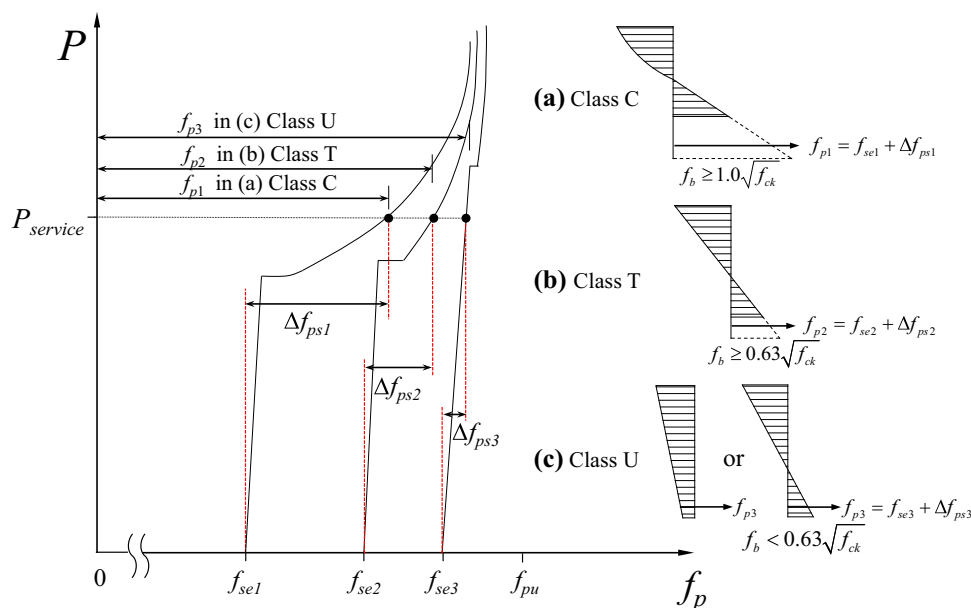


Fig. 1 Class of prestressed concrete sections and effect of effective prestress on Δf_{ps} .

Table 1 Summary of parametric study.

Section of type	Details of section ^a	Tensile strength of strand (f_{ps} , MPa)	Yield strength of reinforcing bar (f_y , MPa)	Effective prestress ratio (f_{pe}/f_{pu})	Reinforcing index (ω)	PPR (%)					
Rectangular	12RB16	1860 (Grade 270)	420 (Grade 60) 550 (Grade 80)	0.5 0.55 0.6 0.65	0.1	50					
	16RB40				0.15	67					
					0.2	100					
					0.25						
					0.3						
					0.35						
					0.4						
					0.45						
					0.5						
					Number of rectangular sections: 432						
Tee	12T16	1860 (Grade 270)	420 (Grade 60) 550 (Grade 80)	0.5 0.55 0.6 0.65	0.0135	50					
	16T40				0.027	67					
					0.0405	100					
					0.054						
					0.0675						
					0.081						
					0.0945						
					0.108						
					Number of T sections: 384						
					Inverted Tee	28IT20	1860 (Grade 270)	420 (Grade 60) 550 (Grade 80)	0.5 0.55 0.6 0.65	0.1	50
40IT52	0.15	67									
	0.2	100									
	0.25										
	0.3										
	0.35										
	0.4										
	0.45										
	0.5										
	Number of inverted T sections: 432										
Total number of analyses: 1248											

^aSectional details can be found in Fig. 2.

considered in the parametric study. In the rectangular or T-shaped sections, the section heights were 400 mm for 12RB16 and 12T16 series, and 1000 mm for 16RB40 and 16T40 series, respectively, while they were 400 and 1321 mm for 28IT20 and 40IT52 series, respectively, in the IT-shaped sections. The reinforcing index (ω) ranged from 0.1 to 0.5 for the rectangular and IT-shaped sections, and from 0.0135 to 0.108 for the T-shaped sections, respectively, where the reinforcing index (ω) can be defined, as follows:

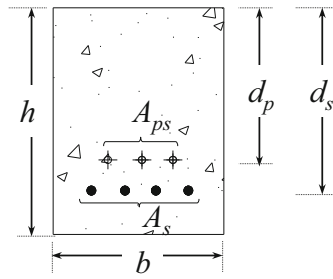
$$\omega = \rho_s f_y / f'_c + \rho_p f_{ps} / f'_c \quad (1)$$

where ρ_s and ρ_p are the tensile reinforcement ratios of nonprestressed and prestressing steels, respectively, f_y is the yield strength of nonprestressed steel, f_{ps} is the ultimate

tensile stress in the prestressing steel at the nominal flexural strength, and f'_c is the compressive strength of concrete. At the initial analysis, the compressive strength of concrete (f'_c) was found to have a negligible effect on the net tensile stress (Δf_{ps}), and thus it was fixed as 40 MPa in this study. In the AASHTO-LRFD bridge design specifications (2010), the partial prestressing ratio (PPR) is defined as follows:

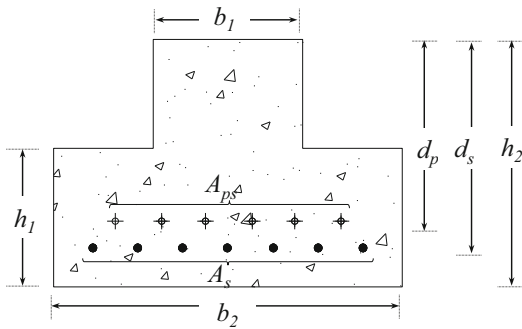
$$PPR(\%) = \frac{A_{ps} f_{ps}}{A_{ps} f_{ps} + A_s f_y} \times 100 \quad (2)$$

where A_{ps} and A_s are the areas of the prestressing and nonprestressed longitudinal tension reinforcements, respectively. In this study, the PPRs of 50, 67, and 100% were considered;



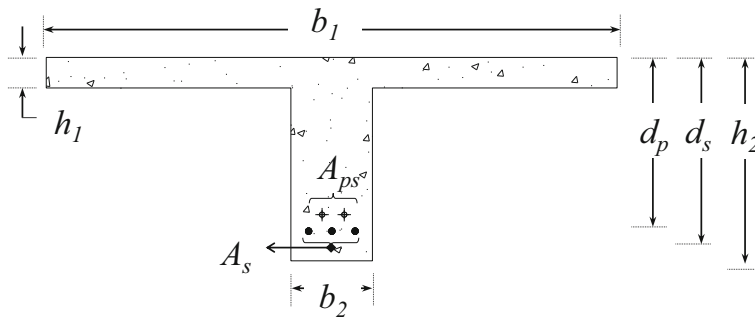
b , in (mm)	h , in (mm)	A_g , in ² (mm ²)	Designation
12 (300)	16 (400)	192 (120000)	RS series
16 (400)	40 (1000)	640 (400000)	RL series

(a)



b_1/b_2 , in (mm)	h_1/h_2 , in (mm)	A_g , in ² (mm ²)	Designation
12 / 28 (300 / 711)	8 / 20 (200 / 400)	368 (237358)	ITS series
24 / 40 (600 / 1000)	16 / 52 (400 / 1321)	1504 (971052)	ITL series

(b)



b_1/b_2 , in (mm)	h_1/h_2 , in (mm)	A_g , in ² (mm ²)	Designation
90 / 12 (2220 / 300)	5 / 16 (120 / 400)	582 (350400)	TS series
110 / 16 (2800 / 400)	6 / 40 (150 / 1000)	1204 (760000)	TL series

(c)

Fig. 2 Dimensional details of analysis members. **a** Details of rectangular section, **b** Details of inverted Tee section, and **c** Details of double Tee section.

PPR = 100% means that it is a full PSC member, and PPR < 100% means that it is a partial PSC member (Nawy 2010; Karayannis and Chalioris 2013). As explained in the bottom of Table 2, the analysis cases were named by four letters that represent sectional shape, section size, reinforcing index, and magnitude of the effective prestress, respectively. For example, RS1A is a PSC member that has rectangular

section, the sectional area of 192 in² (120,000 mm²), the reinforcing index of 0.1, and the effective prestress of 0.5 f_{pu} .

4.2 Stress Estimation of Prestressing Strands in PSC Members Under Service Loads

As shown in Fig. 3, the layered sectional analysis model was utilized in the flexural analyses of the PSC members (Bentz 2000; Kim et al. 2011; Marí et al. 2016). As shown in

Table 2 Description of naming the analysis cases.

Sectional area of concrete (in ²)*				Reinforcing index(ω)			Magnitude of prestress	
Shape Size	R	IT	T	Cases (level)	Reinforcing index (R or IT / T)		Cases (level)	Effective prestress (f_{se}/f_{pu})
					R or IT	T		
S	192	368	582	1	0.1	0.0135	A	0.5
				2	0.15	0.027		
				3	0.2	0.0405		
				4	0.25	0.054	B	0.55
				5	0.3	0.0675		
				6	0.35	0.081		
L	640	1,504	1,204	7	0.4	0.0945	C	0.6
				8	0.45	0.108		
				9	0.5	-	D	0.65
				X				

* Sectional details can be found in Fig. 2.

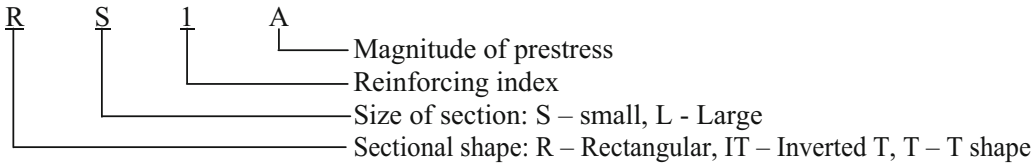


Fig. 4a, the compressive stress–strain model of concrete presented in Vecchio and Collins (1986) was used in this study, as follows:

$$\sigma_c = f'_c \left[2 \left(\frac{\varepsilon_c}{\varepsilon_{ce}} \right) - \left(\frac{\varepsilon_c}{\varepsilon_{ce}} \right)^2 \right] \quad (3)$$

The tensile stress–strain models for concrete before and after cracking can be expressed, respectively, as follows:

$$\sigma_c = E_c \varepsilon_c \quad \text{if } \varepsilon_c \leq \varepsilon_{cr} \quad (4a)$$

$$\sigma_c = \frac{\alpha_1 \alpha_2 f_{cr}}{1 + \sqrt{500 \varepsilon_c}} \quad \text{if } \varepsilon_c > \varepsilon_{cr} \quad (4b)$$

where E_c is the elastic modulus of concrete, f_{cr} is the cracking stress of concrete, and α_1 is the bond factor of tension reinforcements, which is taken to be 1.0 for deformed reinforcing bars, 0.7 for bonded prestressing strands, and $(0.7A_{ps} + 1.0A_s)/(0.7A_{ps} + 1.0A_s)(A_{ps} + A_s)$ for combined reinforcements (Collins and Mitchell 1991). α_2 is a loading coefficient that is taken to be 0.7 for sustained loads. For the stress–strain relationship of nonprestressed reinforcements ($f_s - \varepsilon_s$ relationship), as shown in Fig. 4b, the elasto-plastic model was used (Scholz 1990; Rodriguez-Gutierrez and Aristizabal-Ochoa 2000). The modified Ramberg–Osgood model shown in Fig. 4c was adopted as the stress–strain relationship of the

prestressing strands ($f_p - \varepsilon_p$ relationship), as follows (Mattock 1979; Park et al. 2017):

$$f_p = E_p \varepsilon_p \left\{ A + \frac{(1-A)}{[1 + (B\varepsilon_p)^C]^{1/C}} \right\} \quad (5)$$

where E_p is the elastic modulus of the prestressing strands, and the coefficients A, B, and C are 0.025, 118, and 10, respectively (Devalapura and Tadros 1992). The compressive force of concrete (C_c) was calculated by dividing the cross section into n layers with 5 mm thickness. For the tensile force of concrete, the tension contribution of concrete after cracking, i.e., the so-called tension-stiffening effect, was reflected in the analyses. Therefore, the equilibrium equations on the cross section at an arbitrary loading stage j can be expressed, as follows:

$$C_{c,j} + T_{c,j} + T_{p,j} + T_{s,j} = \sum_{i=1}^n \sigma_{c,j}(y_i) b_i t + f_p A_{ps} + f_s A_s = 0 \quad (6)$$

$$M_j = T_{p,j} d_p + T_{s,j} d_s + \sum_{i=1}^n \sigma_{c,j}(y_i) b_i t y_i \quad (7)$$

where b_i and t are the width and thickness of the i th concrete layer, respectively, and y_i is the distance of the centroid of

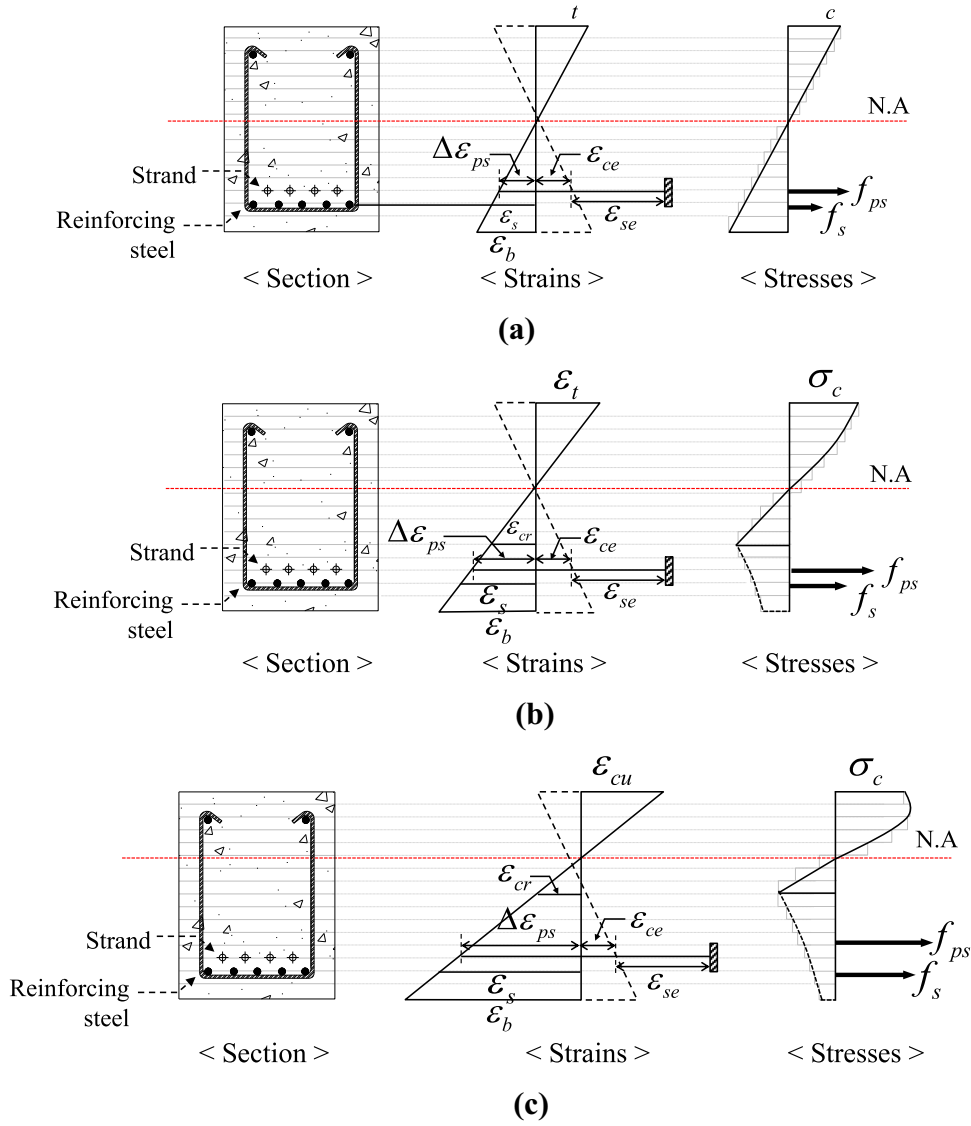


Fig. 3 Sectional analysis of prestressed concrete member. a Uncracked, b Cracked, and c Ultimate.

the i th concrete layer from the extreme top fiber. d_p and d_s are the distance from extreme compression fiber to centroid of prestressing and nonprestressed reinforcements, respectively. When the strain at the extreme compressive fiber of the cross section (ϵ_t) reaches the ultimate strain of concrete (ϵ_{cu}), where ϵ_{cu} was adopted to be 0.003 in this study, the flexural moment calculated by substituting the sectional force components satisfying Eq. (6) into Eq. (7) is defined as the flexural strength (M_n) of the cross section, and two-thirds of this flexural strength was defined as the flexural moment at the service loads ($M_{service}$) (Gagely and Lutz 1968; Frosch 1999; Atutis et al. 2015). In the following discussions, only the Class C sections were considered, excluding the Class U and T sections. In accordance with Tables 24.5.4.1 and 9.6.2.1 in the ACI318-14, if the concrete compressive stress at the service loads exceeds the allowable stress level or M_n is smaller than 1.2 times the cracking moment ($1.2M_{cr}$) due to very low tensile reinforcement ratio, those PSC members were also excluded. The cracking moment M_{cr} was estimated, as follows:

$$M_{cr} = f_r Z_g + f_{se} A_{ps} \left(\frac{r_c^2}{y} + e_p \right) \quad (8)$$

where f_r is the modulus of rupture of concrete, Z_g is the section modulus of gross section, r_c is the radius of gyration, y is the distance of the centroid of the section from the extreme top fiber, and e_p is the eccentricity of prestressing steel from the centroid of the section.

Figure 5 shows the flowchart of computational procedures for calculating Δf_{ps} at the service loads. After $M_{service}$ is determined as two-third of the flexural strength (M_n), the ultimate compressive strain (ϵ_t) is assumed, and the strain at the bottom fiber of the cross section (ϵ_b) is updated until the force equilibrium expressed in Eq. (6) is satisfied. The flexural moment (M_j) at an arbitrary loading stage j can be calculated by substituting the sectional force components estimated from Eq. (6) into Eq. (7), and the same computational procedures are repeated by increasing ϵ_t until M_j reaches $M_{service}$. At the service load ($M_{service}$), the change in tensile stress of prestressing strand (Δf_{ps}) can be estimated, as follows:

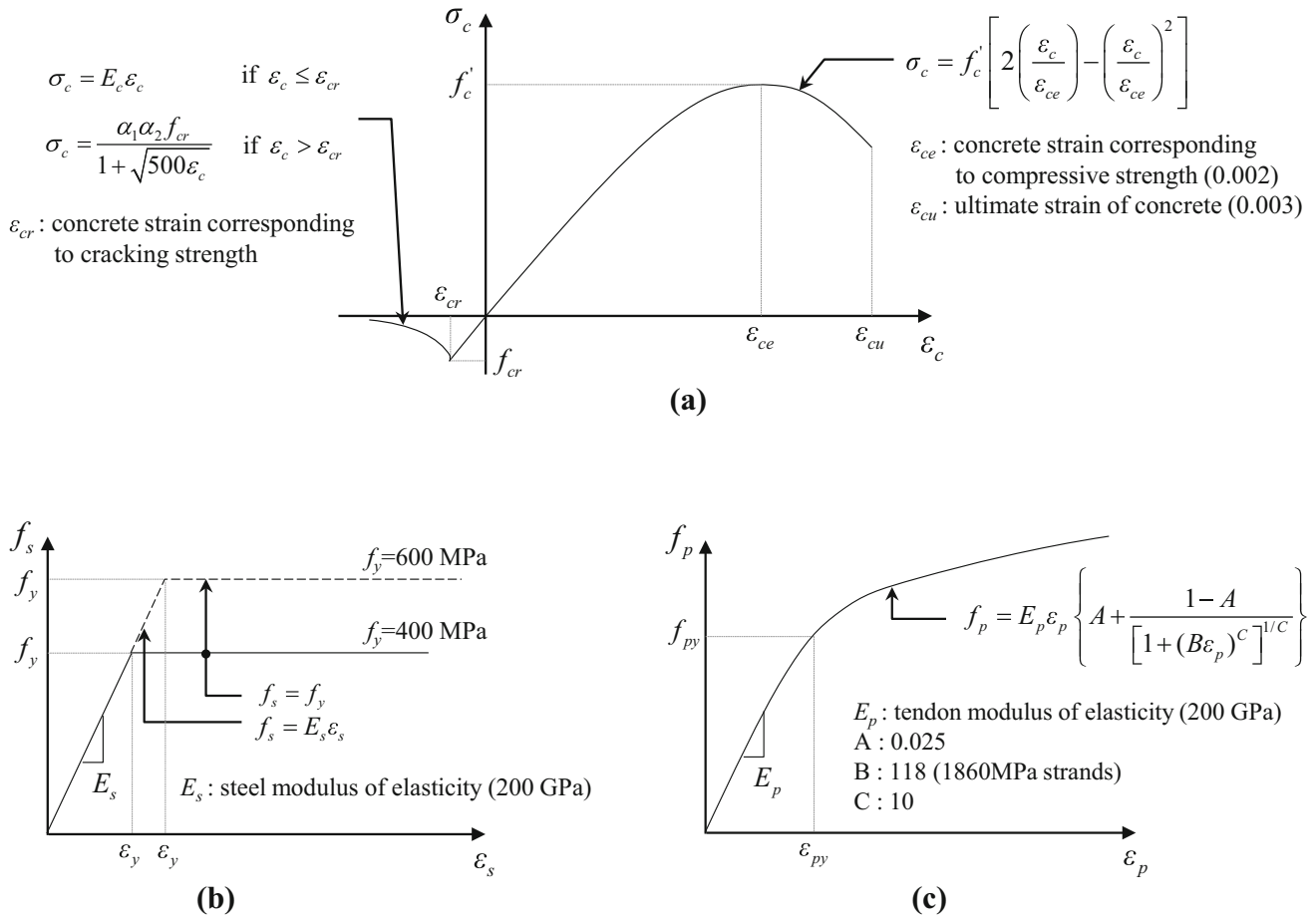


Fig. 4 Flexural behavior analysis. **a** Stress–strain curve of concrete, **b** Stress–strain curve of reinforcing steel, and **c** Stress–strain curve of strand.

$$\Delta f_{ps} = f_{p,service} - f_{dc} \quad (9)$$

where $f_{p,service}$ is the tensile stress in prestressing steel at the service loads, and f_{dc} is the decompression stress, the stress in the prestressing steel when the stress is zero in the concrete at the same level with the centroid of the prestressing steel, which can be computed as follows:

$$f_{dc} = \frac{n A_{ps} f_{se}}{A_c} \left(1 + \frac{e_p}{r_c^2} y \right) + f_{se} \quad (10)$$

where n is the elastic modulus ratio, and A_c is the gross area of the concrete section.

5. Analysis Results of the Parametric Study

5.1 Rectangular Sections

Figure 6 shows the analysis results of the rectangular sections (RS series) with the section size of 300 mm × 400 mm. The vertical axis of the graph is the stress increase in the prestressing steel of the PSC section at the service loads (Δf_{ps}), and the horizontal axis is the reinforcing index (ω). As afore-mentioned, all the analysis results are for the Class C sections, except those shown by the cross marks (×) that are the analysis results for the Class T sections. It can be

seen that the PSC members belong to the Class T category mostly when both the PPRs and the effective prestresses (f_{se}) are high. In all the Class C sections, the Δf_{ps} values were the maximum when the reinforcing index (ω) ranges from 0.1 to 0.2, and decreased nonlinearly outside that range. In the full PSC sections with the PPR 100%, the Δf_{ps} values showed a significantly decreasing trend as the magnitude of the effective prestress (f_{se}) increased, compared to the partial PSC sections. In the partial PSC sections with the PPRs 67 or 50%, the Δf_{ps} values were higher when they were reinforced with 550 MPa reinforcing bars (Grade 80) than those reinforced with 420 MPa reinforcing bars (Grade 60). This is because the longitudinal reinforcement ratio (ρ_s) is relatively lower in the PSC members with 550 MPa reinforcing bars than those with 420 MPa reinforcing bars at the same level of the reinforcing index (ω). Especially, as shown in Fig. 6b, in the partial PSC members with 550 MPa reinforcements and PPR 50%, when the effective prestress (f_{se}) is 0.5 f_{pu} and the reinforcing index (ω) ranges from 0.1 to 0.25, the values of Δf_{ps} exceeded the maximum stress limit of 250 MPa specified in the ACI318-14.

Figure 7a shows the flexural behaviors of the RS1A, RS3A, and RS5A sections with 100% PPR selected from the analysis results presented in Fig. 6, and these sections had the same properties except for the reinforcing index (ω), which were 0.1, 0.2, and 0.3, respectively. The $M_{cr}/M_{service}$

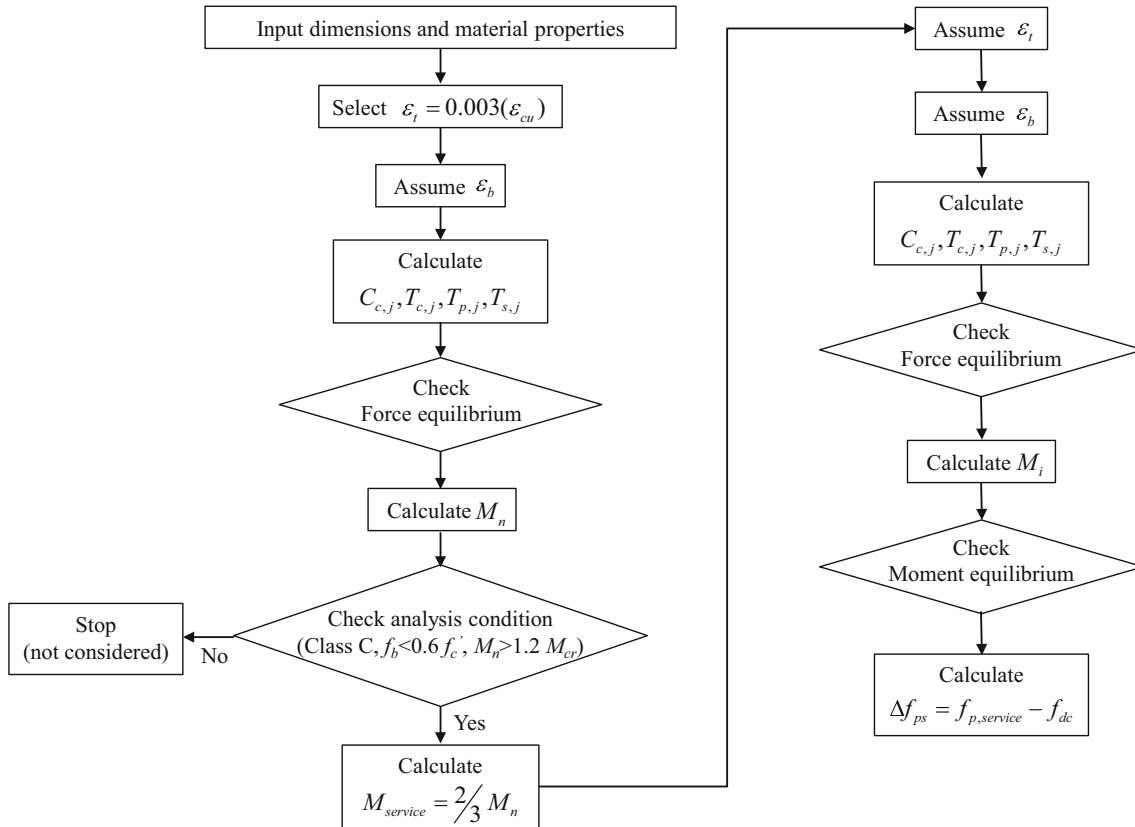


Fig. 5 Computational procedures of flexural analysis.

ratios shown in the top of the graph indicate that the RS3A had the lowest $M_{cr}/M_{service}$ value, which means that the RS3A experienced larger deformations at the service load level. For this reason, the RS3A is expected to have higher Δf_{ps} than the other sections. Figure 7b shows $M_{cr}/M_{service}$ ratios with respect to the reinforcing index (ω) and the PPR. As expected, the $M_{cr}/M_{service}$ ratios increased as the PPR increased, but also exhibited concave-up curve shapes depending on the reinforcing index (ω). This indicates a close correlation between $M_{cr}/M_{service}$ and Δf_{ps} shown in Fig. 6; that is an inversely proportional relationship. The minimum value of $M_{cr}/M_{service}$ in each series, however, appeared in the range of the reinforcing index (ω) from 0.2 to 0.25, which is slightly different from the range of the reinforcing index (ω) where the maximum value of Δf_{ps} appeared, i.e., 0.15 to 0.2.

Figures 8a and b show the analysis results of the RS1A sections with a low reinforcing index ($\omega = 0.1$) and those of the RS7A sections with a high reinforcing index ($\omega = 0.4$), in which each graph shows the flexural behaviors of a partial PSC member with the PPR 50% and a full PSC member with the PPR 100% with respect to Δf_{ps} . As previously explained, the lower the PPR is, the lower the cracking strength (M_{cr}) and the higher the Δf_{ps} values. In addition, the sections with high reinforcing index, i.e., the RS7A series, showed a clear difference in the Δf_{ps} values depending on the magnitude of the PPR.

5.2 Flanged Sections: Inverted T (IT) and T Sections

Figures 9 and 10 show the analysis results of the ITS series and TS series, which are inverted T and T sections, respectively. (See Fig. 2b, c) The ITS series have almost the same flexural strength (M_n) as the RS series with rectangular sections having the same reinforcing index, but the flexural cracking strengths (M_{cr}) of the IT sections are quite higher than those of the rectangular sections. For this reason, the IT sections have higher stiffness at the service loads and thus have lower Δf_{ps} values than the RS series. Also, because the IT sections have higher stiffness at the service loads, many cases in the ITS series were classified into the Class T or U sections, rather than the Class C section. As shown in Fig. 9a and b, in all the ITS series reinforced with 420 or 550 MPa reinforcing bars, the stress increase in prestressing steel (Δf_{ps}) was within the stress limitation of 250 MPa, and the maximum value of Δf_{ps} appeared in the reinforcing index (ω) ranging from 0.2 to 0.3.

As shown in Fig. 10, the stress change (Δf_{ps}) in the full PSC sections with the PPR 100% was more sensitive by the magnitudes of effective prestress (f_{se}) compared to those in the partial PSC sections, which was also observed the same in the analysis results of the rectangular sections. At the same reinforcement ratio, the TS series had lower cracking strength (M_{cr}) than the RS series with the rectangular sections, but their flexural moment at the service loads ($M_{service}$) were similar to the RS series, and thus the TS series showed higher magnitudes of Δf_{ps} compared to the RS series. The maximum values of Δf_{ps} were estimated in the reinforcing

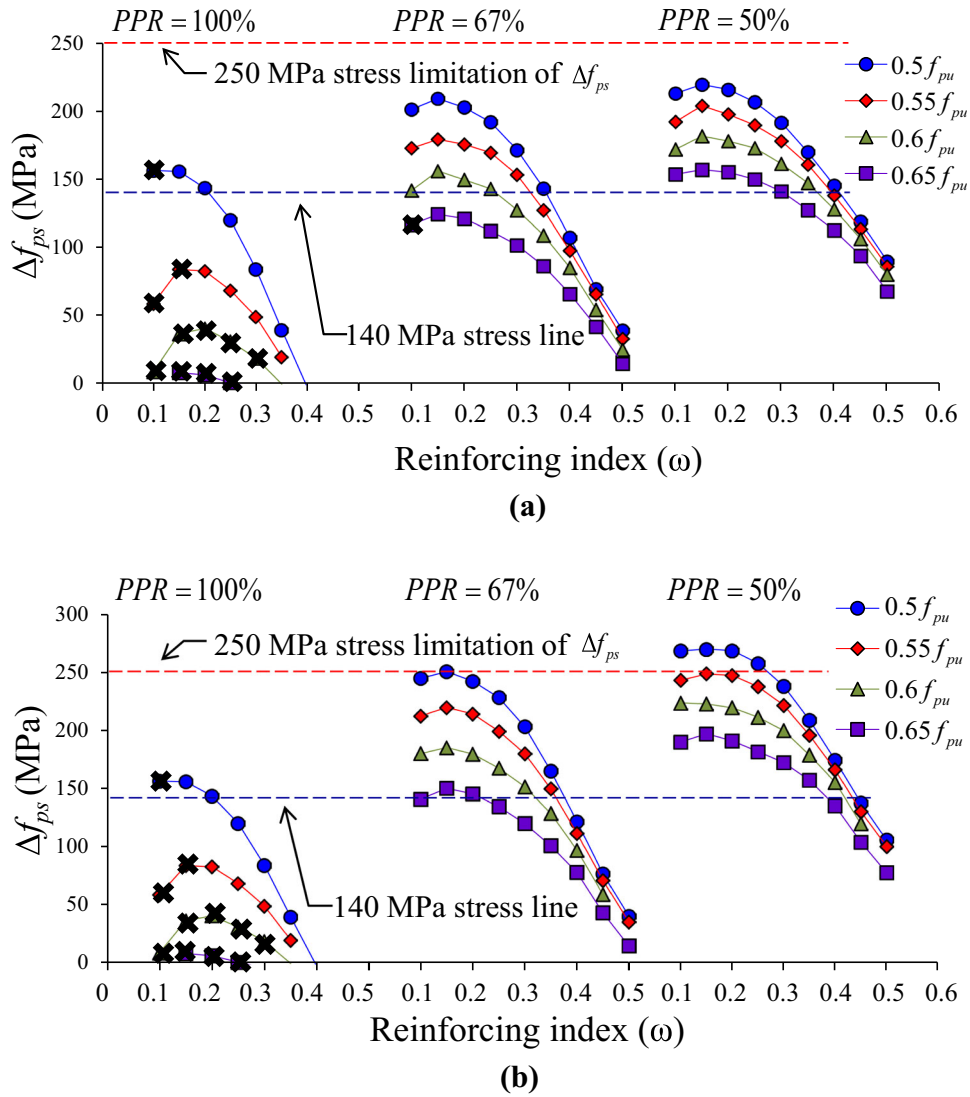


Fig. 6 Analysis results for rectangular sections. **a** RS series with 420 MPa non-prestressed reinforcement and **b** RS series with 550 MPa non-prestressed reinforcement.

index (ω) ranging from 0.04 to 0.06, after which it gradually decreased. In addition, it can be seen that the Δf_{ps} values of the partially prestressed TS sections are larger when the yield strengths of nonprestressed steel are greater. In particular, as shown in Fig. 10b, in the case of the partial PSC members reinforced with 550 MPa nonprestressed steel and the PPR 67%, the magnitudes of Δf_{ps} exceeded the maximum stress limit of 250 MPa specified in the ACI318-14 when the effective prestress (f_{se}) was $0.5 f_{pu}$ and the reinforcing index (ω) was greater than 0.025. For the partial PSC members reinforced with 550 MPa reinforcements and the PPR 50%, the magnitudes of Δf_{ps} also exceeded the 250 MPa limit when the effective prestress (f_{se}) was less than $0.55 f_{pu}$ and the reinforcing index (ω) was more than 0.025

5.3 Effects of Tension Stiffening and Section Size

It is expected that the effects of the tension stiffening on the flexural strengths of PSC members are marginal because the post-cracking resistance of concrete clearly decreases as the flexural crack width increases; however, it can still play

an important role in the service load behavior (Collins and Mitchell 1991; Sahamitmongkol and Kishi 2011; Patel et al. 2016). Figures 11a and b show the effect of the tension stiffening on the stress behaviors of the prestressing strands at the service loads. The effect of the tension stiffening on Δf_{ps} was greater in the full PSC members than that in the partial PSC members with PPR 50%. Especially, as shown in Fig. 11c, the contribution of the concrete in the cracked tension zone to the flexural strength (M_{tc}/M_n) is larger in the PSC sections with low reinforcing index. Accordingly, if the tension stiffening effect is not taken into account, Δf_{ps} can be overestimated in the PSC sections, which would be more serious in those with low tension reinforcement ratios. Therefore, in this study, the tension stiffening effect was considered in the estimations of Δf_{ps} shown in Figs. 6, 7, 8, 9 and 10. Figure 12a shows a comparison of Δf_{ps} values of the RS series with the section height of 400 mm and the RL series with the height of 1000 mm. As the section size increases, the magnitude of Δf_{ps} slightly increases, but their differences were very small. Figure 12b shows a comparison of Δf_{ps} values between the TS series with the height of

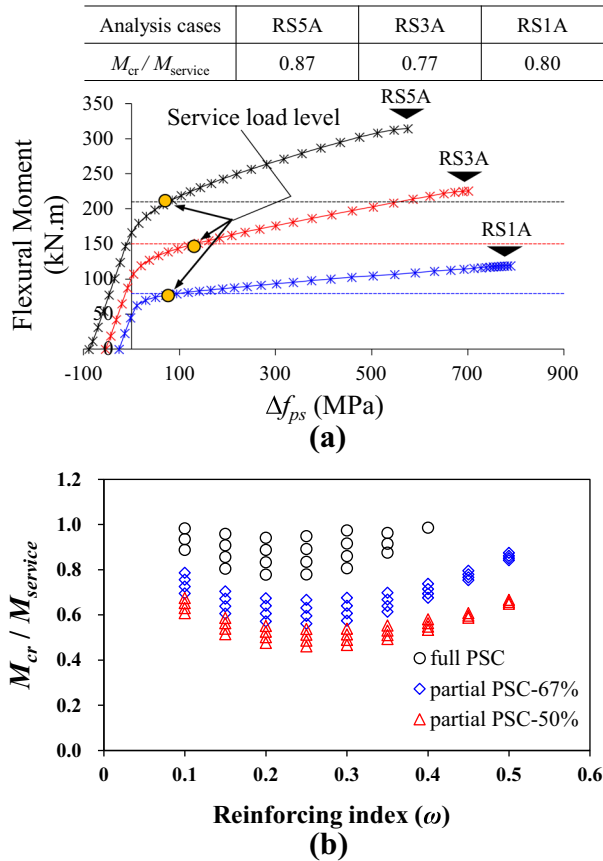


Fig. 7 Effect of reinforcing index on Δf_{ps} . **a** Effect of reinforcing index on Δf_{ps} of selected sections and **b** Effect of reinforcing index and PPR on $M_{cr}/M_{service}$.

400 mm and TL series with the height of 1000 mm. The differences in Δf_{ps} depending on the section sizes were negligible except the sections with the low reinforcing index under about 0.02. The reason of the large differences in Δf_{ps} between the TS and TL series for the sections with the low reinforcing index is because the neutral axis depths are inevitably small in these members due to the low reinforcing ratio, leading to be cracked in flexure at the service loads. After cracking, high tensile strains are developed in the prestressing strands, and thus high levels of Δf_{ps} are also expected. A similar tendency was also found in the analysis results of the IT sections, as shown in Fig. 12c.

6. Proposed Approaches

6.1 Simple Checking of the Net Tensile Stress

Table 3 shows the minimum magnitude of the effective prestress ($f_{se,min}$) required to satisfy 250 MPa stress limit ($\Delta f_{ps,allow}$) specified in the ACI318 code based on the parametric study results shown in Figs. 6, 9, and 10. As expressed by the red horizontal lines in Fig. 6, if the magnitude of the effective stress (f_{se}) is greater than $0.55 f_{pu}$, the stress increase of the prestressing strands at the service loads (Δf_{ps}) in all the full and partial PSC members with the rectangular sections can be well controlled within 250 MPa. In addition, as shown in Fig. 9, if the effective prestress (f_{se})

is greater than $0.5 f_{pu}$, Δf_{ps} can be also controlled to be under 250 MPa for all the cases in the inverted T sections regardless of the grades of the nonprestressed reinforcements.

As shown in Fig. 10, in the case of the T-shaped sections, the minimum effective prestress ($f_{se,min}$) can be determined as $0.5 f_{pu}$ for all the full PSC members and the partial PSC members except the partial PSC members with 550 MPa reinforcements. For the partial PSC members with 550 MPa reinforcements, the minimum effective prestress ($f_{se,min}$) is $0.60 f_{pu}$ to meet the Δf_{ps} limit of 250 MPa.

The current ACI318-14 building code allows to use $2/3 f_y$ for both 420 and 550 MPa reinforcing bars as the steel stress at the service loads when the maximum allowable spacing (s_{max}) of the flexural reinforcements is checked for the proper crack control. Soltani et al. (2013) and Harries et al. (2012) also demonstrated that $2/3 f_y$ can be taken as the stress in the steel reinforcements at the service loads (f_s) for the high yield strength steels even up to 827 MPa (120,000 psi). Therefore, it is considered that the allowable stress increase of the prestressing steel under the service load ($\Delta f_{ps,allow}$) can be increased from 250 to 350 MPa in the partial PSC members reinforced with 550 MPa nonprestressed steel. In that case, the minimum magnitude of the effective prestress ($f_{se,min}$) can be $0.5 f_{pu}$ for all the partial PSC members reinforced with 550 MPa nonprestressed steel.

6.2 Simple Method for Calculating the Net Tensile Stress (Δf_{ps})

The ACI318-14 code provides the maximum allowable spacing of flexural reinforcements (s_{max}) to control the flexural crack width at the service load, as follows:

$$s_{max} = \eta \left[380 \left(\frac{280}{f_s} \right) - 2.5c_c \right] \leq \eta 300 \left(\frac{280}{f_s} \right) \quad (11)$$

where η is the modification coefficient for the member types, which is 1.0 for RC members, $2/3$ for full PSC members, and $5/6$ for partial PSC members. In addition, f_s is the tensile stress of the nonprestressed reinforcements, and Δf_{ps} is applied for the PSC members instead of the f_s value. However, if Δf_{ps} is less than 140 MPa, there is no requirement to check the maximum spacing (s_{max}) of the flexural reinforcements even for the Class C PSC members. As aforementioned, the current ACI318-14 Code permits to use $2/3 f_y$ (≈ 370 MPa) for the f_s in Eq. (11) even for the RC members with the Grade 80 reinforcements ($f_y = 550$ MPa), and therefore, the same principle can be applied to the allowable Δf_{ps} value (i.e., $\Delta f_{ps,allow}$) for the partial PSC members reinforced with the Grade 80 reinforcements ($f_y = 550$ MPa). This study, therefore, suggests that $\Delta f_{ps,allow}$ can be 350 MPa for the partial PSC members with 550 MPa nonprestressed steels, while it is 250 MPa for the full PSC members and the partial PSC members reinforced with 420 MPa nonprestressed steels. Figure 13 shows a comparison of the maximum spacings of flexural reinforcements (s_{max}) calculated from Eq. (11) against the cover thickness

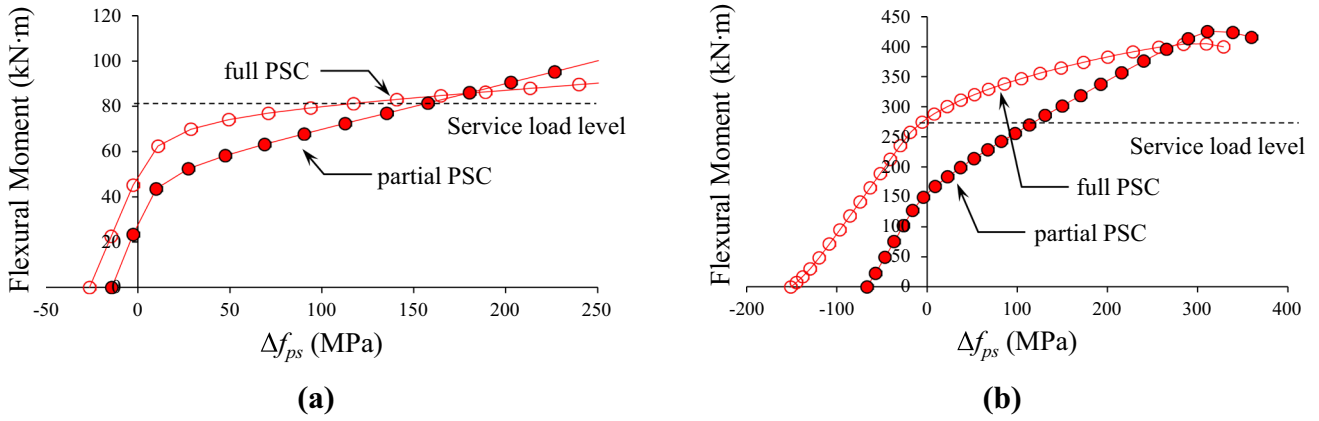


Fig. 8 Effect of partial prestressing ratio on Δf_{ps} . **a** PSC members with a low level of reinforcing index (RS1A series) and **b** PSC members with a high level of reinforcing index (RS7A series).

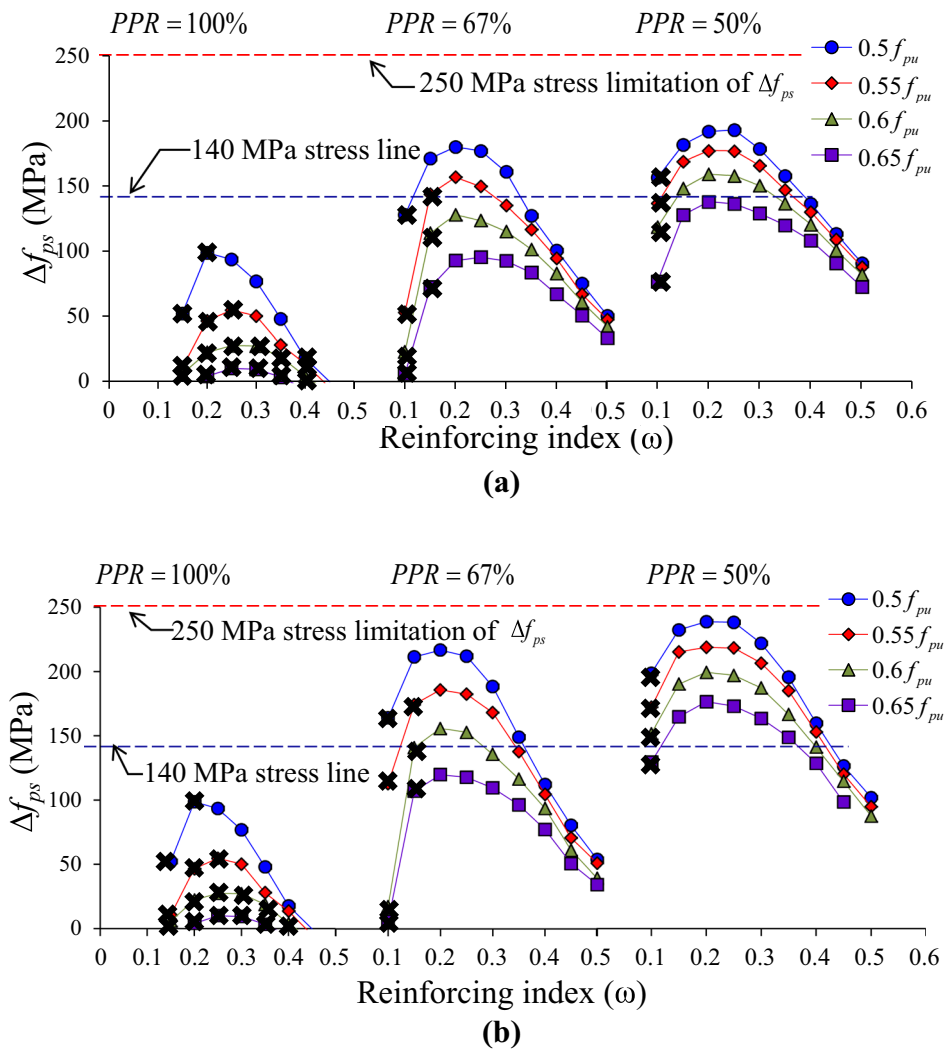


Fig. 9 Analysis results of inverted Tee sections. **a** ITS series with 420 MPa nonprestressed reinforcement and **b** ITS series with 550 MPa nonprestressed reinforcement.

(c_c), where the effect of member types and the grade of nonprestressed reinforcements are also presented. Except some cases of the partial PSC members reinforced with 420 MPa nonprestressed steel having the concrete cover depth over 60 mm or the full PSC members having the concrete cover depth over 120 mm, the allowable spacing of

the tension reinforcements were always smaller in the PSC members than in the RC members. In particular, the allowable spacing of the tension reinforcements in the PSC members reinforced with 550 MPa nonprestressed reinforcements is always smaller than those reinforced with 420 MPa nonprestressed reinforcements.

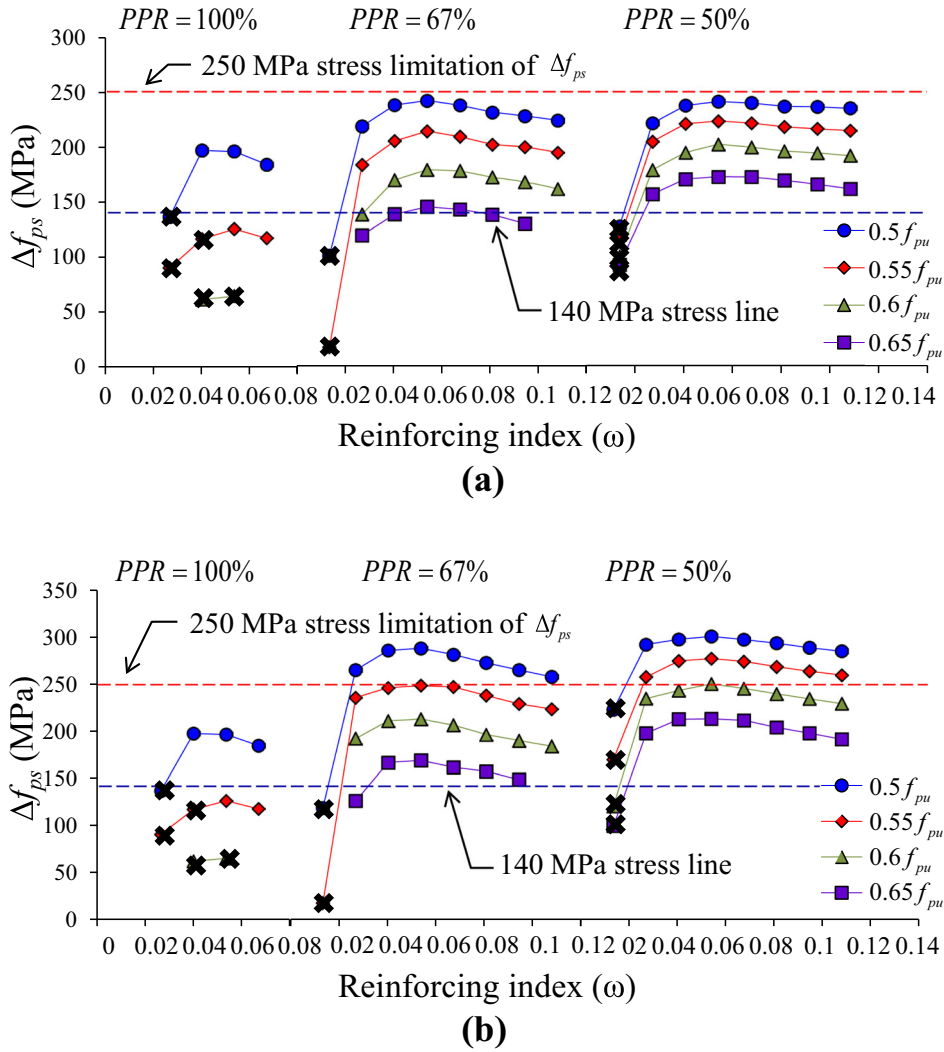


Fig. 10 Analysis results of Tee sections. **a** TS series with 420 MPa nonprestressed reinforcement and **b** TS series with 550 MPa nonprestressed reinforcement.

As summarized in Table 3, when the effective prestress (f_{se}) is greater than $0.50 f_{pu}$, which would be the case in most PSC members, the stress increase of prestressing strands (Δf_{ps}) in all the full PSC members (PPR = 100%) satisfies the 250 MPa stress limit ($\Delta f_{ps,allow}$) specified in the ACI318-14. As aforementioned, in the partial PSC members (PPR $\geq 50\%$) with the effective prestress (f_{se}) greater than $0.50 f_{pu}$, the maximum allowable stress of the prestressing strand at the service load ($\Delta f_{ps,allow}$) is 250 MPa if 420 MPa nonprestressed steel is used, while it is 350 MPa if 550 MPa nonprestressed steel is used. In order to satisfy the 250 MPa stress limit ($\Delta f_{ps,allow}$) in the partial PSC members (PPR $\geq 50\%$) with 550 MPa nonprestressed steel, however, the effective prestress (f_{se}) shall be greater than $0.55 f_{pu}$, $0.60 f_{pu}$, and $0.50 f_{pu}$ for the rectangular, T-shaped, and IT-shaped sections, respectively. Thus, it is very important to apply a proper magnitude of the effective prestress (f_{se}) to satisfy the stress limit ($\Delta f_{ps,allow}$) for the serviceability design of the PSC members. If the Δf_{ps} value is, however, smaller than the stress limit ($\Delta f_{ps,allow}$), it is not necessary to use the maximum value of Δf_{ps} (i.e., $\Delta f_{ps,allow}$) in the Eq. (11) for calculating the maximum spacing of flexural reinforcements

(s_{max}). In that case, the Δf_{ps} value can be used as f_s in Eq. (11), by which more economical designs can be achieved. As mentioned above, however, the cracked section analysis, which requires complex iterative calculations (Lee and Kim 2011; ACI Committee 318 2014), need to be conducted to estimate Δf_{ps} of the Class C PSC members. Thus, this study also aimed at proposing a simple method to estimate Δf_{ps} for the Class C PSC members.

Figure 14 shows the moment-tendon stress ($M - f_p$) curve of the Class C PSC member that has cracks at the service loads, and the stress in the prestressing steel at the flexural cracking moment ($f_{p,cr}$) can be calculated, as follows:

$$f_{p,cr} = f_{se} + n \frac{M_{cr} e}{I_g} = f_{se} + \frac{E_p M_{cr} e}{E_c I_g} \quad (12)$$

In addition, the Class C PSC member typically shows a nonlinear behavior after flexural cracking and undergoes a significant reduction in stiffness after flexural cracking. Thus, as shown in Fig. 14, if the sectional moment-tendon stress behavior curve is assumed to be linear in the post-cracking region, the stress in the prestressing steel at the service loads ($f_{p,service}$) can be calculated, as follows:

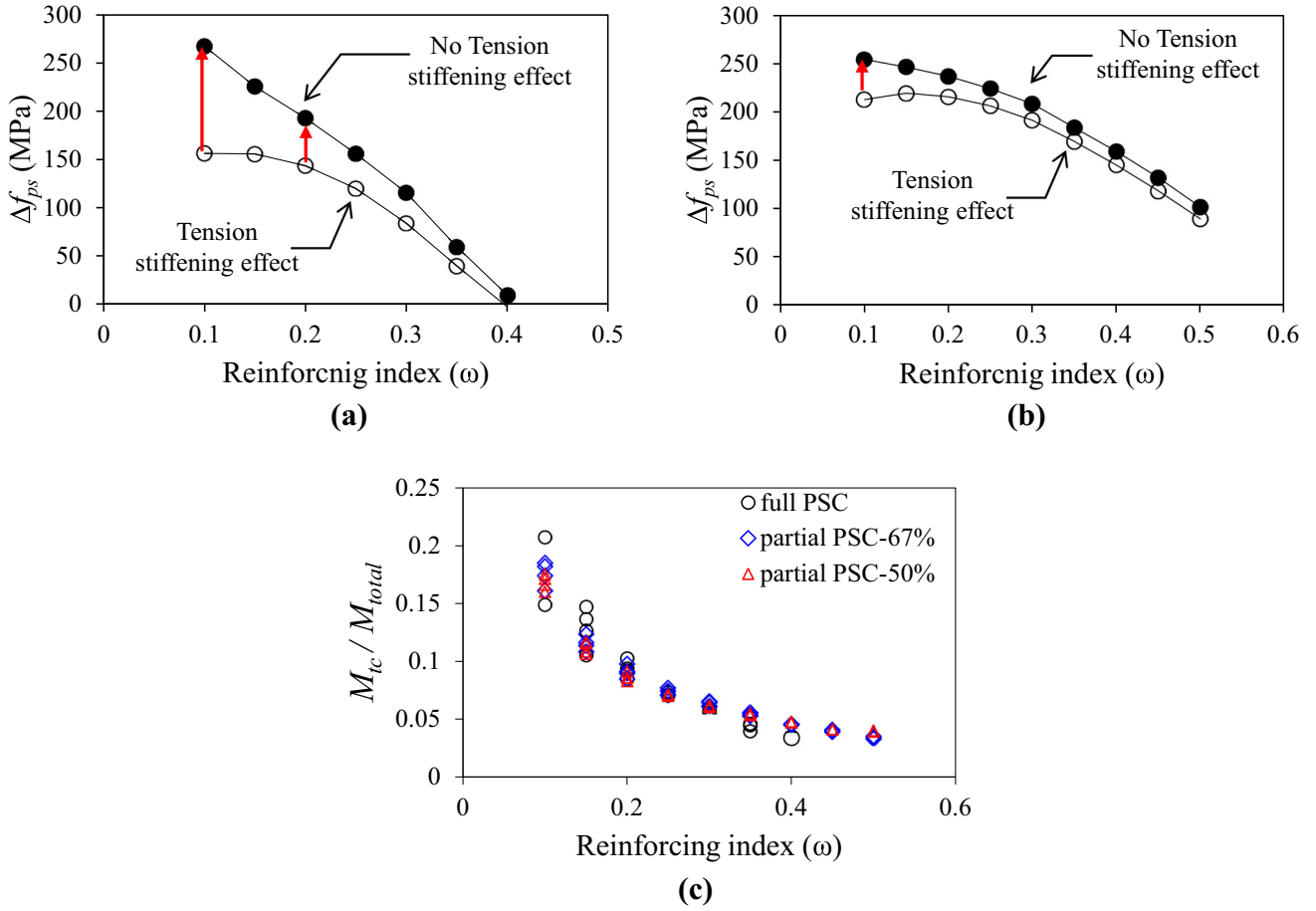


Fig. 11 Effect of tension stiffening on Δf_{ps} . **a** Full PSC sections, **b** Partial PSC sections (PPR = 50%), and **c** Contribution of concrete in tension zone to flexural strength.

Table 3 Minimum effective prestress ($f_{se,min}$) to satisfy the tensile stress limit ($\Delta f_{ps,allow}$).

Section shapes	PPR 100% ($\Delta f_{ps} \leq 250$ MPa)	Partially prestressed concrete members (PPR $\geq 50\%$)		
		$f_y = 420$ MPa (for $\Delta f_{ps} \leq 250$ MPa)	$f_y = 550$ MPa (for $\Delta f_{ps} \leq 250$ MPa)	$f_y = 550$ MPa (for $\Delta f_{ps} \leq 350$ MPa)
R	$0.50 f_{pu}$	$0.50 f_{pu}$	$0.55 f_{pu}$	$0.50 f_{pu}$
T	$0.50 f_{pu}$	$0.50 f_{pu}$	$0.60 f_{pu}$	$0.50 f_{pu}$
IT	$0.50 f_{pu}$	$0.50 f_{pu}$	$0.50 f_{pu}$	$0.50 f_{pu}$

$$f_{p,service} = \frac{M_{service} - M_{cr}}{M_n - M_{cr}} (f_{ps} - f_{p,cr}) + f_{p,cr} \quad (13)$$

Then, the net tensile stress increase of the prestressing strands (Δf_{ps}) can be calculated, as follows:

$$\Delta f_{ps} = f_{p,service} - f_{dc} \quad (14)$$

For the further simplification of the calculation of Δf_{ps} , both $f_{p,cr}$ and f_{dc} in Eqs. (13) and (14) can be approximated as f_{se} , and Eq. (14) then becomes:

$$\Delta f_{ps} = \frac{2/3 M_n - M_{cr}}{M_n - M_{cr}} (f_{ps} - f_{se}) \quad (15)$$

The ACI318-14 code presents a simplified method to calculate the ultimate tensile stress of the prestressing strands (f_{ps}), as follows:

$$f_{ps,ACI} = f_{pu} \left\{ 1 - \frac{\gamma_p}{\beta_1} \left(\rho_p \frac{f_{pu}}{f'_c} + \frac{d_s f_y}{d_p f'_c} (\rho_s - \rho'_s) \right) \right\} \quad (16)$$

where γ_p is the factor used for type of prestressing reinforcement, β_1 is the factor for the depth of equivalent rectangular compressive stress block to the depth of neutral axis, and ρ'_s is the reinforcement ratio in compression. For a practical application, if the ultimate stress of the prestressing strands ($f_{ps,ACI}$) calculated from Eq. (16) and its corresponding flexural moment of the section ($M_{n,ACI}$) are substituted into Eq. (15), the simplified net tensile stress of

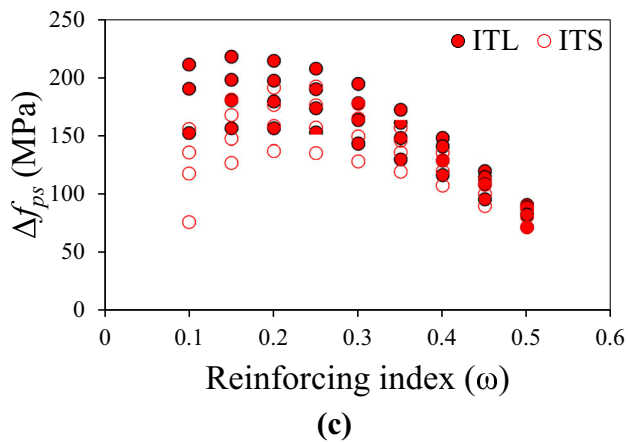
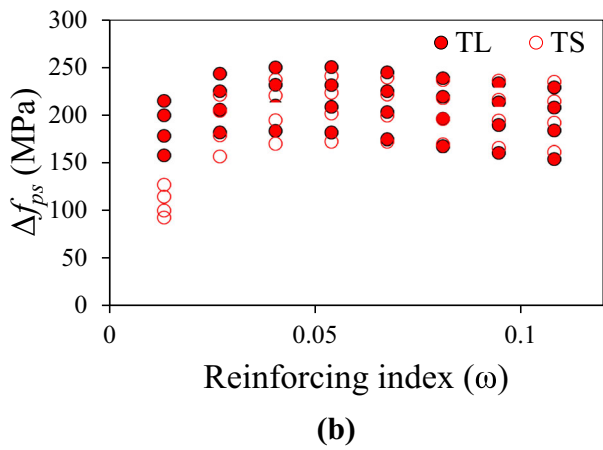
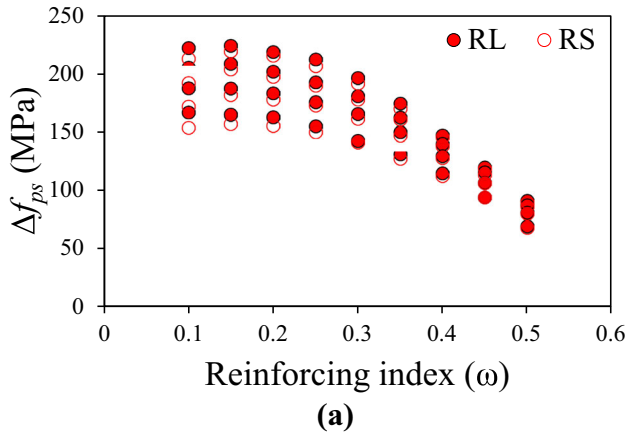


Fig. 12 Difference of Δf_{ps} according to the size of section, **a** Rectangular section, **b** Tee section, and **c** Inverted Tee section.

the prestressing strands ($\Delta f_{ps,ACI}$) can be expressed, as follows:

$$\Delta f_{ps,ACI} = \frac{2/3 M_{n,ACI} - M_{cr}}{M_{n,ACI} - M_{cr}} (f_{ps,ACI} - f_{se}) - \kappa f_{se} \leq \Delta f_{ps,allow} \quad (17)$$

where κ is the calibration factor, which is 0.03 for rectangular sections and 0.05 for T- or IT-shaped sections. Figure 15 shows a comparison of $\Delta f_{ps,ACI}$ for the Class C

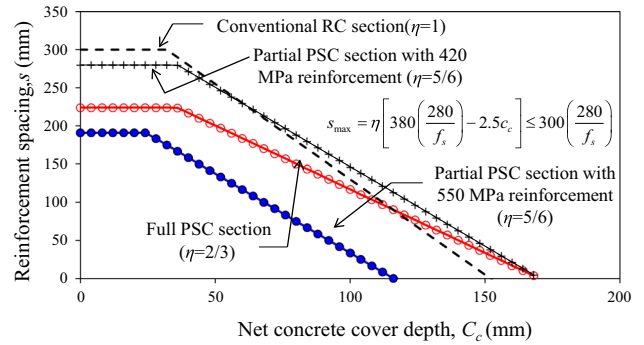


Fig. 13 Maximum allowable spacing of flexural reinforcement.

sections at the service loads estimated by Eq. (17) and those obtained from nonlinear flexural analyses (Δf_{ps}). The net tensile stress of the prestressing strands ($\Delta f_{ps,ACI}$) obtained from Eq. (17) provided more conservative analysis results compared to those estimated by the nonlinear flexural analyses. The simplified net tensile stress ($\Delta f_{ps,ACI}$) estimated by Eq. (17) showed a fairly good accuracy level of up to about 250 MPa, whereas the differences between $\Delta f_{ps,ACI}$ and Δf_{ps} become larger when Δf_{ps} is greater than 250 MPa. This is of course due to the assumptions introduced to simplify the calculation process. Nevertheless, the simplified equation proposed in this study is for the design purposes, and all the Δf_{ps} values calculated by the simple equation are conservative, which means that it can be utilized as a useful alternative method for the design purposes.

Figure 16 shows a flowchart for calculating the maximum allowable spacing of the flexural reinforcement (s_{max}) for the crack control design of the PSC members proposed in this study. After performing an elastic analysis for the PSC section, if the stress in the precompressed extreme tension fiber at the service loads (f_b) belongs to the Class C category, the design effective prestress (f_{se}) is then compared with the minimum required effective prestress ($f_{se,min}$) presented in Table 3. If the minimum required effective prestress condition is satisfied, i.e., $f_{se} \geq f_{se,min}$, Eq. (17) can be used to calculate $\Delta f_{ps,ACI}$, and if $\Delta f_{ps,ACI}$ does not exceed 140 MPa, it is not necessary to check the spacing of the tension reinforcements for the crack control design. On the other hand, If $\Delta f_{ps,ACI}$ exceeds 140 MPa, the maximum spacing of the flexural reinforcement (s_{max}) can be calculated by substituting $\Delta f_{ps,allow}$ or $\Delta f_{ps,ACI}$ into f_s in Eq. (11), and the spacing of the flexural reinforcement (s) can be then determined not to exceed the maximum spacing (s_{max}), where $\Delta f_{ps,allow}$ can be taken to be 250 MPa for the full PSC members or the partial PSC members with 420 MPa nonprestressed steel, and 350 MPa for the partial PSC members with 550 MPa nonprestressed steel. If the minimum required effective prestress condition is not satisfied, i.e., $f_{se} < f_{se,min}$, however, detailed check should be performed through the cracked section analysis, or the section should be redesigned, if necessary.

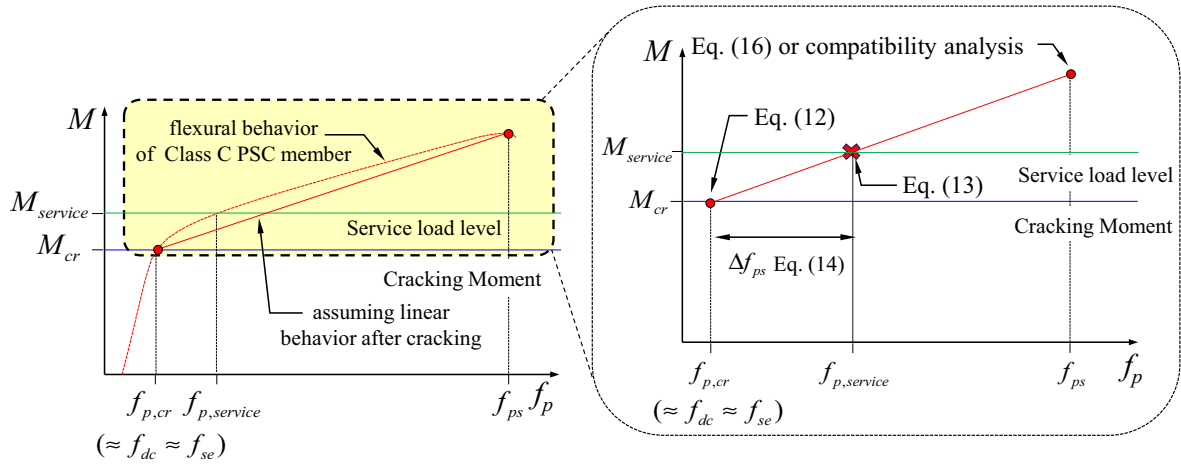


Fig. 14 Concept of the simple method to calculate Δf_{ps} .

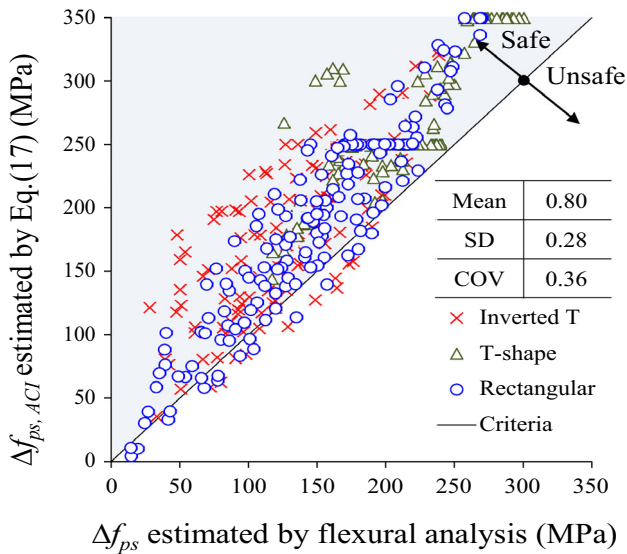


Fig. 15 Comparison of analysis results by simple and detailed method.

7. Conclusions

In this study, the nonlinear flexural analyses were conducted on 1248 prestressed concrete (PSC) sections with the various section shapes, section sizes, partial prestressing ratios, reinforcing indices, yield strengths of the nonprestressed reinforcements, and effective prestresses. Based on the flexural analysis results, a simple method for estimating the net tensile stress of prestressing strands under service loads (Δf_{ps}) was proposed, by which proper spacings of the tension reinforcements in PSC members can also be obtained. On the other hand, a summary table was also proposed, which can be used to easily check whether the net tensile stress (Δf_{ps}) exceeds the specified stress limit (250 or 350 MPa) under the service loads using only the magnitude of the effective prestress (f_{se}) without calculating the net tensile stress of the prestressing strands (Δf_{ps}). From this study, the following conclusions can be drawn:

(1) The nonlinear flexural analysis results of the PSC members showed that the net tensile stress of

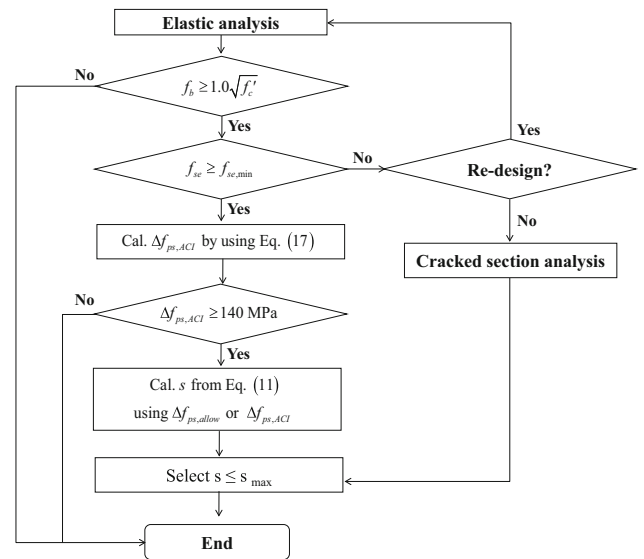


Fig. 16 Determination procedure for the maximum spacing of flexural reinforcement (s_{max}).

prestressing strands at the service load (Δf_{ps}) increases as the yield strength of the nonprestressed reinforcement is greater and as the partial prestressing ratio (PPR) or the effective prestress level (f_{se}) decreases. It also appeared that the stress change in Δf_{ps} is more sensitive in the full PSC members compared to in the partial PSC members with respect to the magnitude of the effective prestress (f_{se}).

- (2) In the full PSC members (PPR = 100%) with the effective prestress (f_{se}) greater than $0.50 f_{pu}$, which would be the case in most PSC members, the stress increase (Δf_{ps}) of prestressing strands satisfied the 250 MPa stress limit ($\Delta f_{ps,allow}$) specified in the ACI318-14.
- (3) For the RC members with 550 MPa reinforcing bars as well as 420 MPa reinforcing bars, the current ACI318-14 code permits to use $2/3 f_y$ as the steel stress in the calculation of the maximum spacing of the flexural reinforcement (s_{max}) for proper crack control; therefore, it is considered that the allowable tensile stress increase of the prestressing steels under the service loads

($\Delta f_{ps,allow}$) can be increased from 250 to 350 MPa in the partial PSC members with 550 MPa reinforcing bars.

- (4) In the partial PSC members ($PPR \geq 50\%$) with an effective prestress (f_{se}) greater than $0.50 f_{pu}$, the maximum Δf_{ps} satisfies the 250 MPa stress limit when 420 MPa reinforcing bar is used, and it satisfies the 350 MPa stress limit when 550 MPa reinforcing bar is used. To satisfy 250 MPa stress limit ($\Delta f_{ps,allow}$) in the partial PSC members ($PPR \geq 50\%$) with 550 MPa reinforcing bar, however, the effective prestress (f_{se}) shall be greater than $0.55 f_{pu}$, $0.60 f_{pu}$, and $0.50 f_{pu}$ for the rectangular, T-shaped, and IT-shaped sections, respectively.
- (5) A summary table was proposed, which can be used to easily check whether the net tensile stress (Δf_{ps}) exceeds the specified stress limit (250 or 350 MPa) under the service loads using only the magnitude of the effective prestress (f_{se}), requiring no complex cracked section analysis, and it can be thus easily applied in practice.
- (6) The simplified method proposed in this study for estimating the net tensile stress of the prestressing strands (Δf_{ps}) in the Class C PSC sections under the service loads provided conservative analysis results compared to those estimated through the nonlinear flexural analyses, and it is expected to be a useful alternative method for the serviceability design of the PSC members.
- (7) Since the proposed design method was developed by utilizing non-linear flexural analyses, it is considered that experimental evidences are required for the confirmation of the proposed methods.

Acknowledgements

This work was supported by the 2016 Research Fund of the University of Seoul.

Open Access

This article is distributed under the terms of the Creative Commons Attribution 4.0 International License (<http://creativecommons.org/licenses/by/4.0/>), which permits unrestricted use, distribution, and reproduction in any medium, provided you give appropriate credit to the original author(s) and the source, provide a link to the Creative Commons license, and indicate if changes were made.

References

ACI Committee 318. (2014). *Building code requirements for structural concrete (ACI 318-14) and commentary*. Farmington Hills, MI: American Concrete Institute.

- American Association of State Highway and Transportation Officials. (2010). *AASHTO LEFD bridge design specifications: Customary U.S. units* (5th ed.). Washington, D.C.: AASHTO.
- Atutis, M., Valivonis, J., & Atutis, E. (2015). Analysis of serviceability limit state of GFRP prestressed concrete beams. *Composite Structures*, 134(15), 450–459.
- Bentz, E.C. (2000). *Sectional analysis of reinforced concrete members*. Ph.D. Dissertation, University of Toronto, Ontario, Canada.
- Collins, M. P., & Mitchell, D. (1991). *Prestressed concrete structures*. Englewood Cliffs, NJ: Prentice Hall.
- Devalapura, R. K., & Tadros, M. K. (1992). Stress-strain modeling of 270 ksi low-relaxation prestressing strands. *PCI Journal*, 37(2), 100–106.
- Frosch, R. J. (1999). Another look at cracking and crack control in reinforced concrete. *ACI Structural Journal*, 99(3), 437–442.
- Gagely, P., & Lut, L. (1968). Maximum cracks width in reinforcement concrete flexural member. *ACI Special Publication SP-20*, 20, 87–117.
- Harries, K. A., Shahrooz, B. M., & Soltani, A. (2012). Flexural crack widths in concrete girders with high-strength reinforcement. *Journal of Bridge Engineering*, 17(1), 29–57.
- Karayannis, C. G., & Chalioris, C. E. (2013). Design of partially prestressed concrete beams based on the cracking control provisions. *Engineering Structures*, 48(1), 402–416.
- Kim, K. S., & Lee, D. H. (2011). Flexural behavior of prestressed composite beams with corrugated web: Part II. Experiment and verification. *Composite Part B: Engineering*, 42(1), 1617–1629.
- Kim, K. S., Lee, D. H., Choi, S. M., Choi, Y. H., & Jung, S. H. (2011). Flexural behavior of prestressed composite beams with corrugated web: Part I. Development and analysis. *Composite Part B: Engineering*, 42(6), 1603–1616.
- Lee, D. H., Hwang, J. H., Kim, K. S., Kim, J. S., Chung, W., & Oh, H. (2014). Simplified strength design method for allowable compressive stress in pretensioned concrete members at transfer. *KSCE Journal of Civil Engineering*, 18(7), 2209–2217.
- Lee, D. H., & Kim, K. S. (2011). Flexural strength of prestressed concrete members with unbonded tendons. *Structural Engineering Mechanics*, 38(5), 675–696.
- Lee, J. Y., Lee, D. H., Hwang, J. H., Park, M. K., Kim, Y. H., & Kim, K. S. (2013). Investigation on allowable compressive stresses in pre-tensioned concrete members at transfer. *KSCE Journal of Civil Engineering*, 17(5), 1083–1098.
- Marí, A., Bairán, J. M., Cladera, A., & Oller, E. (2016). Shear design and assessment of reinforced and prestressed concrete beams based on a mechanical model. *Journal of Structural Engineering*, 142(10), 1–17.
- Mast, R. F., Dawood, M., Rizkalla, S. H., & Zia, P. (2008). Flexural strength design of concrete beams reinforced with high-strength steel bars. *ACI Structural Journal*, 105(5), 570–577.
- Mattock, A. H. (1979). Flexural strength of prestressed concrete sections by programmable calculator. *PCI Journal*, 24(1), 32–54.

- Nawy, E. G. (2010). *Prestressed concrete: A fundamental approach* (5th ed.). Upper Saddle River, NJ: Pearson Prentice Hall, Pearson Education Inc.
- Park, H., & Cho, J. Y. (2017). Ductility analysis of prestressed concrete members with high-strength strands and code. *ACI Structural Journal*, 114(34), 407–416.
- Park, H., Jeong, S., Lee, S. C., & Cho, J. Y. (2016). Flexural behavior of post-tensioned prestressed concrete girders with high-strength strands. *Engineering Structures*, 112(1), 90–99.
- Park, J. H., Park, H., & Cho, J. Y. (2017). Prediction of stress in bonded strands at flexural. *ACI Structural Journal*, 114(56), 697–705.
- Patel, K. A., Chaudhary, S., & Nagpal, A. K. (2016). A tension stiffening model for analysis of RC flexural members under service load. *Computers and Concrete*, 17(1), 29–57.
- Prestressed Concrete Institute. (2010). *PCI design handbook: Precast and prestressed concrete*. Chicago, IL: Precast/Prestressed Concrete Institute.
- Rodriguez-Gutierrez, J. A., & Aristizabal-Ochoa, J. D. (2000). Partially and fully prestressed concrete sections under biaxial bending and axial load. *ACI Structural Journal*, 97(4), 553–563.
- Sahamitmongkol, R., & Kishi, T. (2011). Tension stiffening effect and bonding characteristics of chemically prestressed concrete under tension. *Materials and Structures*, 44(2), 455–474.
- Scholz, H. (1990). Ductility, redistribution, and hyperstatic moments in partially prestressed members. *ACI Structural Journal*, 87(3), 341–349.
- Skogman, B. C., Tadros, M. K., & Grasmick, R. (1988). Flexural strength of prestressed concrete members. *PCI Journal*, 33(5), 96–123.
- Soltani, A., Harries, K. A., & Shahrooz, B. M. (2013). Crack opening behavior of concrete reinforced with high strength reinforcing steel. *International Journal of Concrete Structures and Materials*, 7(4), 253–264.
- Vecchio, F. J., & Collins, M. P. (1986). The modified compression-field theory for reinforced concrete elements subjected to shear. *ACI Journal*, 83(2), 219–231.